J. Phys. B: At. Mol. Opt. Phys. **32** (1999) 2267–2276. Printed in the UK PII: S0953-4075(99)01319-X

Breit–Pauli and intermediate-coupling collision strengths for the correlation resonances that arise in the electron-impact excitation of Ni^{4+}

N R Badnell† and D C Griffin‡

† Department of Physics and Applied Physics, University of Strathclyde, Glasgow G4 0NG, UK
‡ Department of Physics, Rollins College, Winter Park, FL 32789, USA

Received 27 January 1999

Abstract. We present the results of *R*-matrix Breit–Pauli and intermediate-coupling frame transformation (ICFT) calculations for the electron-impact excitation of Ni^{4+} at low energies. We focus on the correlation resonances due to the $3p^5 3d^8$ configuration, which are a severe test of the ICFT method. We observe differences between the results of the two methods for the detailed shape and position of the broad correlation resonances but the effect of using the Breit–Pauli method is mainly redistributive, except for extremely weak transitions. This observation, together with our previous findings (Griffin *et al* 1998 *J. Phys. B: At. Mol. Opt. Phys.* **31** 3713–27), means that the ICFT method is expected to be an accurate way of allowing for relativistic effects in the electron-impact excitation of complex ions, particularly for rate coefficients for the spectroscopic modelling of astrophysical plasmas.

1. Introduction

Electron-impact excitation of complex (open-shell) ions, such as ions of the transition metals, is a key process for diagnosing many laboratory and astrophysical plasmas. Large numbers of target states are required both to allow for coupling between levels, and to obtain accurate atomic structure via a large configuration-interaction (CI) basis. Furthermore, relativistic effects can be expected to be significant here ($Z > 20$). The importance of the contribution from resonances to the rate coefficient for many transitions makes the *R*-matrix method the optimal close-coupling (CC) theory to use. New algorithms to treat d-shells efficiently, and associated computer codes to implement them, have been developed by Burke *et al* (1994). These codes (RMATRX II) are non-relativistic. Whilst a Breit–Pauli version could be developed, as has been done for RMATRX I—see Berrington *et al* (1995), an alternative approach is possible based on an intermediate-coupling frame transformation (ICFT), see Griffin *et al* (1998).

The ICFT method is based on an initial non-relativistic solution to the scattering problem and a multi-channel quantum defect theory (MQDT) solution in the outer region, i.e. outside of the *R*-matrix box, which treats all closed channels as open (see Badnell *et al* 1998). The unphysical *K*-matrix is transformed to intermediate coupling using term-coupling coefficients — since all channels are treated as open, the severe difficulties encountered with transforming the physical *K*-matrix at closed-channel energies is avoided (Griffin *et al* 1998). In addition, the use of a frame transformation ensures that Rydberg series converge on non-degenerate level energies rather than term energies. A similar approach can be taken with photoionization, but there the unphysical dipole matrices are transformed as well, see Gorczyca *et al* (1998). The

0953-4075/99/092267+10$19.50

advantage of an ICFT calculation over a full Breit–Pauli calculation arises primarily from the fact that it employs the non-relativistic $(N + 1)$-electron Hamiltonian in LS-coupling, rather than the much larger Breit–Pauli $(N+1)$-electron Hamiltonian in intermediate coupling. Therefore, Breit–Pauli calculations are often an order of magnitude more demanding than ICFT calculations and, since there appears to be no end in sight with respect to the size of the problems of current interest, the ICFT method allows one to tackle many problems that might be otherwise intractable.

However, one aspect of the ICFT method that has yet to be studied is how it fares when correlation resonances are present. These arise from $(N+1)$-electron configurations explicitly added to the total wavefunction for the electron–ion system, both to satisfy the orthogonality requirement and to allow for short-range correlation effects so as to partially offset the use of a non-converged N-electron eigenstate expansion. We expect correlation resonances to be a severe test of the ICFT method for the following reasons: (i) standard MQDT does not factor-out the energy dependence of such resonances (this applies to our Breit–Pauli MQDT calculations as well); (ii) no frame transformation is applied here and so the core levels are degenerate, this is in addition to the usual neglect by the ICFT method of the nuclear spin–orbit interaction with the Rydberg electron which is likely to be most noticeable for low-lying resonances; and (iii) the transformation to intermediate coupling using term-coupling coefficients is based on a core of N-electrons that are inequivalent to the $(N + 1)$th electron — correlation resonances frequently involve equivalent electrons.

In this paper we report on both Breit–Pauli and ICFT results for the electron-impact excitation of transitions within the ground configuration of Ni^{4+}. This system has been studied recently in LS-coupling by Teng *et al* (1998). They observed large, broad, correlation resonances in a number of transitions and so this system is an ideal one to study the accuracy of the ICFT method in the severe circumstances noted above. The outline of the remainder of this paper is as follows: in section 2 we review the relevant theory, in section 3 we look at its specific application to Ni^{4+}, in section 4 we present our results, and we finish in section 5 with a short conclusion.

2. Theory

The total $(N + 1)$-electron R-matrix wavefunction, Ψ_E, in the inner region can be expanded in terms of basis functions, Ψ_k, at any energy E as (Burke and Robb 1975)

$$\Psi_E = \sum_k A_{Ek} \Psi_k, \tag{1}$$

where the expansion coefficients A_{Ek} are ultimately determined by the R-matrix, and the basis functions can be expanded as

$$\Psi_k = \mathcal{A} \sum_{ij}^{\prime} c_{ijk} \Phi_i u_{ij}(r) + \sum_l \mathrm{d}_{lk} \phi_l. \tag{2}$$

The Φ_i are N-electron (atomic) eigenstates and the u_{ij} are continuum basis orbitals which are taken to be orthogonal to the atomic basis orbitals. The ϕ_l are $(N + 1)$-electron states formed from the atomic basis orbitals and they are added to ensure completeness of the basis functions Ψ_k, given the orthogonality condition. It is these ϕ_l that give rise to the correlation resonances, so-called because a large ϕ_l set can model short-range electron–electron correlation effects. The c_{ijk} and d_{lk} coefficients are determined by diagonalizing the $(N+1)$-electron Hamiltonian in the inner region, the eigenvalues and eigenvectors of which determine the (low-lying) poles and surface amplitudes of the R-matrix. $\mathcal{A}$ is the anti-symmetrization operator. The sum

over bound and the integral over continuum N-electron atomic eigenstates in (2) can only be made to converge for the simplest of systems by using, say, Laguerre basis states to discretize the continuum (and further discretize closely-spaced bound states) as implemented in the convergent close coupling (CCC) method (Bray and Stelbovics 1992) and R-matrix with pseudo-states (RMPS) method (Bartschat *et al* 1996). Thus, we have a further motivation for wanting to be able to use as large an N-electron eigenstate expansion as possible, and the use of LS-coupling for the $(N + 1)$-electron Hamiltonians facilitates this.

To obtain the reactance K-matrix, and hence the collision strength and cross section, the inner region radial wavefunctions for each channel i are matched on the R-matrix boundary (at $r = a$) to the outer region solutions. This leads to, in matrix notation,

$$\boldsymbol{\mathcal{K}} = -(\boldsymbol{C} - \boldsymbol{R}\boldsymbol{C}')^{-1}(\boldsymbol{S} - \boldsymbol{R}\boldsymbol{S}') \qquad \text{at} \quad r = a, \tag{3}$$

where $'$ denotes the spatial derivative, $\boldsymbol{R}$ is the R-matrix and the $\boldsymbol{S}$ and $\boldsymbol{C}$ functions are first order perturbations of s and c such that (Seaton 1985)

$$\boldsymbol{S}(r) \underset{r\to\infty}{\sim} s(r) \qquad \text{and} \qquad \boldsymbol{C}(r) \underset{r\to\infty}{\sim} c(r), \tag{4}$$

where s and c are (diagonal matrices of) the usual Coulomb functions (Seaton 1983). The perturbation of s and c is due to the long-range non-Coulomb multipole potentials in the outer region (see also Berrington *et al* 1987). If equation (3) is only applied to open channels then the usual physical K-matrix is obtained. We also solve for the perturbed $\boldsymbol{S}$ and $\boldsymbol{C}$ functions for all closed channels (Badnell *et al* 1998). The s and c functions are then divergent (but only the finite part of the perturbation integrals is retained, see Gorczyca *et al* (1996)). The physical K-matrix is obtained by requiring the elimination of the divergence from the unphysical K-matrix (Seaton 1983):

$$\boldsymbol{K} = \boldsymbol{\mathcal{K}}_{\rm oo} - \boldsymbol{\mathcal{K}}_{\rm oc}\left[\boldsymbol{\mathcal{K}}_{\rm cc} + \tan(\pi\nu)\right]^{-1}\boldsymbol{\mathcal{K}}_{\rm co}, \tag{5}$$

where the matrices are partitioned by open (o) and closed (c) channels, ν denotes the effective quantum numbers and $\tan(\pi\nu)$ is a diagonal matrix. This is all that is required for a Breit–Pauli or LS-coupling calculation. The ICFT method has a further step between equations (3) and (5). The unphysical LS-coupling K-matrix is transformed first to jK-coupling,

$$\boldsymbol{\mathcal{K}}^{jK} \longleftarrow \mathbf{U}_1^{\rm T}\boldsymbol{\mathcal{K}}^{LS}\mathbf{U}_1, \tag{6}$$

by an algebraic recoupling matrix, $\mathbf{U}_1$ — see Griffin *et al* (1998). ($\boldsymbol{\mathcal{K}}^{jK}$ can also be closed-off via equation (5) to obtain, subsequently, purely jK-recoupled level-resolved cross sections.) Second, the unphysical jK-coupling K-matrix is transformed to intermediate coupling,

$$\boldsymbol{\mathcal{K}}^{\rm IC} \longleftarrow \mathbf{U}_2^{\rm T}\boldsymbol{\mathcal{K}}^{jK}\mathbf{U}_2, \tag{7}$$

using a term-coupling matrix, $\mathbf{U}_2$ (see Griffin *et al* 1998, Jones 1975). In addition, calculated or observed level energies are used in the evaluation of the channel energies—this is the frame transformation (see e.g. Aymar *et al* 1996). The advantage of using an MQDT approach for LS-coupling, ICFT or Breit–Pauli calculations is that the solution in the outer region need only take place at a small number of energies ($\sim$100) since the unphysical K-matrix is (usually) slowly varying with energy and so it is amenable to simple interpolation onto the much finer energy mesh that is necessary to delineate detailed resonance structures. An additional advantage that is realized with the ICFT method is that the transformation only takes place on the coarse energy mesh; furthermore, since all channels are treated as open, the large errors that can arise on transforming only the open–open part of the physical K-matrix at closed-channel energies are avoided (see Griffin *et al* (1998) for a detailed discussion). However, one drawback to the ICFT method, compared to the Breit–Pauli method, is that it neglects the nuclear spin–orbit interaction of the $(N + 1)$th electron. This effect is largest on low-lying resonances.

But in the case of correlation resonances the level splitting of the 'core' term energies is also omitted as no frame transformation is applied. Furthermore, the term-coupling transformation matrix is based on a diagonalization of the N-electron target Hamiltonian (see Jones 1975) but the $(N + 1)$th electron in a correlation configuration is frequently equivalent to one in the N-electron target and the use of a transformation based on the N-electron target is questionable. More generally, low-n resonances, whether they are treated as correlation or not, probe the accuracy of the ICFT method because of the possibility of a strong interaction between the $(N + 1)$th electron and the N-electron core, which is not modelled by the term-coupling transformation matrix. The case of equivalent electrons is just the most extreme example.

Finally, we note that the second term on the r.h.s. of equation (5) factors-out the energy dependence of resonances associated with closed-channel functions arising from the first expansion on the r.h.s. of equation (2), the surface amplitudes of which are non-vanishing. The correlation resonances (due to the second expansion on the r.h.s. of equation (2)) are fully contained within the R-matrix box, i.e. have negligible surface amplitudes, and they are described by $\boldsymbol{\mathcal{K}}_{\rm oo}$ which is, thus, rapidly varying with energy. (Although, we note that such resonances are usually very broad, relatively speaking.) Within the framework of the streamlined eigenchannel R-matrix method (Greene and Kim 1988), Lecomte *et al* (1994) have analysed how the resonant and non-resonant parts of $\boldsymbol{\mathcal{K}}_{\rm oo}$ (actually, $\boldsymbol{\mathcal{S}}_{\rm oo}$) can be separated. Our approach is to simply use a sufficiently fine energy mesh to minimize interpolation error to the desired level—with no interpolation of $\boldsymbol{\mathcal{K}}_{\rm oo}$ the 'problem' does not arise.

3. Application to Ni^{4+}

We focus on transitions within the $3p^6 3d^6$ ground configuration of Ni^{4+}. This LS-mixes strongly with the $3p^4 3d^8$ configuration. We used the SUPERSTRUCTURE (Eissner *et al* 1974) subset of AUTOSTRUCTURE (Badnell 1986) to determine our atomic structure. We included both the $3p^6 3d^6$ and $3p^4 3d^8$ configurations in our description of the Ni^{4+} atomic structure. We used nl-dependent Thomas–Fermi–Dirac–Amaldi statistical model potentials to determine the radial orbitals. The scaling parameters, λ_{nl}, were taken to be unity in the determination of the 1s, 2s and 2p radial orbitals while the remainder were determined simultaneously by minimizing the average energy of all (16) terms of the $3p^6 3d^6$ configuration. This resulted in the following values, for λ_{nl}, of 1.070 76, 1.055 02 and 1.046 21 for nl = 3s, 3p and 3d, respectively. In table 1, we present our calculated energies for the 34 levels of the ground configuration and compare them with observed ones taken from Kelly (1987). (We note that our term energies differ from those of Teng *et al* (table 2, 1998) by an amount that is much smaller than the difference from the observed, weighted over fine structure.) We note that some of the term labels on the levels are merely that, labels. They are, in fact, highly mixed. For example, level 9, labelled $^3H_4$, is actually 36% $^3F_4$ and 41% $^3H_4$ while level 11, labelled $^3F_4$, is actually 53% $^3H_4$ and only 31% $^3F_4$. We shall see the consequences of this later.

In our LS-coupling, and hence jK-coupling, calculation the calculated term energies were adjusted to the observed energies, weighted over fine structure, by adjusting the diagonal of the $(N + 1)$-electron Hamiltonian (see, e.g., Berrington *et al* 1995); similar adjustments were made for the levels in our Breit–Pauli calculation. The prescription for our ICFT calculation is a little more subtle. The inner region calculation proceeds as in a normal LS-coupling run, including adjustment of the term energies. The term-coupling coefficients are determined from a separate run using the calculated term and level energies. Thus, in addition to the (optional) replacement of the calculated level energies with the observed for the frame transformation, the calculated term energies must also be replaced with the observed before the intermediate coupling transformation is applied because the LS-coupling K-matrix data will be indexed by

Table 1. Energies in Rydbergs of the lowest 34 levels of Ni^{4+}, relative to the ground level, all from the $3p^63d^6$ configuration.

Index	Level	Theory	Observed[a]	Index	Level	Theory	Observed[a]
1	$^5D_4$	0.0000	0.0000	18	$^1I_6$	0.4324	0.3759
2	$^5D_3$	0.0085	0.0081	19	$^3D_2$	0.4206	0.3793
3	$^5D_2$	0.0143	0.0136	20	$^3D_1$	0.4207	0.3800
4	$^5D_1$	0.0179	0.0171	21	$^3D_3$	0.4236	0.3820
5	$^5D_0$	0.0197	0.0188	22	$^1G_4$	0.4144	0.3846
6	$^3P_2$	0.2581	0.2383	23	$^1S_0$	0.4459	0.4347
7	$^3H_6$	0.2864	0.2471	24	$^1D_2$	0.5030	0.4429
8	$^3H_5$	0.2901	0.2513	25	$^1F_3$	0.5964	0.5278
9	$^3H_4$	0.2891	0.2539	26	$^3P_0$	0.6745	0.6082
10	$^3P_1$	0.2835	0.2615	27	$^3P_1$	0.6828	0.6155
11	$^3F_4$	0.2962	0.2654	28	$^3F_2$	0.6898	0.6254
12	$^3F_3$	0.2978	0.2695	29	$^3F_4$	0.6915	0.6262
13	$^3P_0$	0.2925	0.2701	30	$^3F_3$	0.6924	0.6275
14	$^3F_2$	0.3012	0.2725	31	$^3P_2$	0.6996	0.6302
15	$^3G_5$	0.3431	0.3031	32	$^1G_4$	0.7934	0.7099
16	$^3G_4$	0.3504	0.3104	33	$^1D_2$	1.0533	0.9516
17	$^3G_3$	0.3534	0.3136	34	$^1S_0$	1.3284	—

[a] Kelly (1987).

the observed term order while, initially, the term-coupling coefficients are still indexed by the calculated energy order. To put it more simply, if observed term energies are used in (STG3 of) the LS-coupling calculation, then the same energies must be used to index the transformation to intermediate coupling. (Strictly speaking, this is only necessary if the term order changes.)

As is well known, the use of observed energy levels relative to the ground level does not change the position of the $(N + 1)$-electron correlation levels. The correlation configurations used here are $3p^63d^7$, $3p^53d^8$ and $3p^43d^9$. The first is non-autoionizing while the last is situated well above our energy range of interest. As noted by Teng *et al* (1998), it is the $3p^53d^8$ configuration that gives rise to the correlation resonances that are the focus of the present work. There is little in the way of observed level energies relating to autoionizing levels; but, fortunately in this case, the $3p^53d^8$ correlation resonances are situated far enough above the ionization limit for changes in position, comparable to the differences between theory and observation (see table 1), to be unimportant for the present study.

Our inner-region calculations were carried out using codes that were originally based on the published version of RMATRX I (Berrington *et al* 1995). Since we are focusing on low energies, and to keep the Breit–Pauli calculation tractable, we used ten continuum basis orbitals per orbital angular momentum in all of our calculations. Our LS-coupling, and hence jK-coupling, calculation included the 16CC terms from the $3p^63d^6$ configuration and the 57CI terms that arise from using the $3p^43d^8$ CI configuration as well. Our Breit–Pauli calculation used the corresponding 34CC and 93CI levels. The use of different sized CC and CI expansions assumes that there is negligible coupling to the states that are included in the CI expansion, but not in the CC expansion—we denote this set CI′. The requirement of the ICFT method is subtly different. In addition to requiring that this coupling be negligible, spin–orbit mixing between the CC terms and the CI′ terms must also be negligible because spin–orbit mixing is not taken into account until the K-matrices are transformed. However, this is a very good approximation since spin–orbit mixing between configurations is normally very small; indeed, in our Ni^{4+} problem, renormalization of the term-coupling coefficients for the CC terms, due

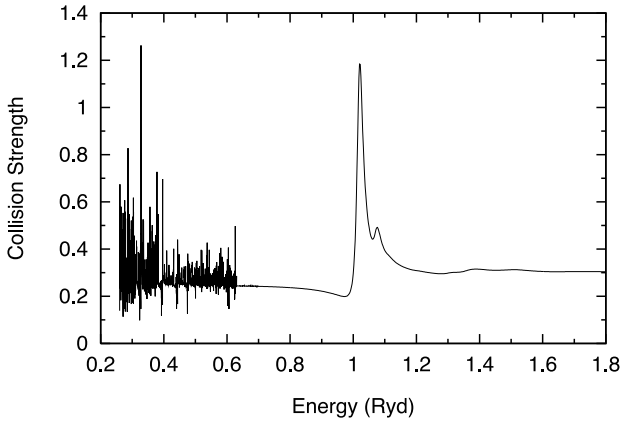

Figure 1. Breit–Pauli R-matrix electron-impact excitation collision strength for the transition $^5D_4-^3P_2$ in Ni^{4+}.

to the neglect of term-coupling coefficients for the CI′ terms, changes the former by less than one part in 10^4. Even if this were not the case, a 57CC term ICFT calculation (which models a 93CC level Breit–Pauli calculation) still only gives rise to at most 170 channels per $LS\pi$ symmetry while the 34CC levels give rise to as many as 201 channels per $J\pi$ symmetry. Finally, we carried out our LS-coupling calculation up to $L = 11$ to enable us to generate jK-coupling and intermediate-coupling results up to $J = 17/2$, which was also the highest J included in our Breit–Pauli calculation.

Our outer region calculations were carried-out with our MQDT version (Badnell *et al* 1998) of Seaton's unpublished STGF code. We included both dipole and quadrupole perturbing potentials—these change the background collision strengths by no more than a few per cent for the strongest transitions considered and by ∼20% for the weakest; resonance shapes and positions are affected correspondingly. This is all that is required to complete the Breit–Pauli calculation. The transformations etc, required to complete our jK-coupling and ICFT calculations, as detailed in section 2, were carried out using the (STGIC) code of Griffin *et al* (1998).

4. Results

In figures1 and 2 we present out Breit–Pauli collision strengths for the $^5D_4-^3P_2$ and $^5D_4-^3H_6$ transitions in Ni^{4+}. All energies are relative to the ground level. Above ∼1 Ryd, we observe the broad correlation resonances that arise in the $^4D^o_J$ and $^4G^o_J$ partial waves and which are very similar to those observed in LS-coupling by Teng *et al* (1998). We used 551 points (without interpolation) over 0.7–1.8 Ryd to map-out this structure. We also note that the narrow resonance structure below ∼0.6 Ryd is mapped-out efficiently using MQDT (equation (5)). We used 221 points initially over 0.26–0.7 Ryd and interpolated the unphysical K-matrix at 2201 points. The accuracy of the ICFT method for this type of resonance has been studied by Griffin *et al* (1998, 1999)—it is very accurate—and so we focus on the correlation resonances.

In figure 3 we compare out Breit–Pauli results with our jK-coupling and ICFT results for the same transitions. The Breit–Pauli peaks are about 0.06 Ryd lower in energy and a little broadened and shifted compared to the jK-coupling and ICFT results, which are barely distinguishable. We note a splitting starting to appear in the peak of the Breit–Pauli results at 1 Ryd. This splitting is probably due to nuclear spin–orbit interactions of the 3p-electrons

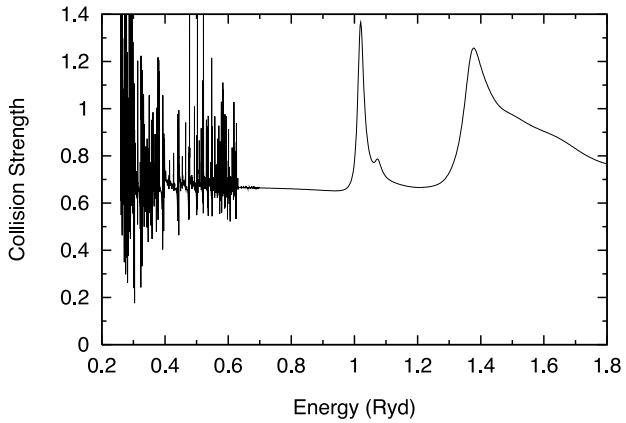

Figure 2. Breit–Pauli R-matrix electron-impact excitation collision strength for the transition $^5D_4-^3H_6$ in Ni^{4+}.

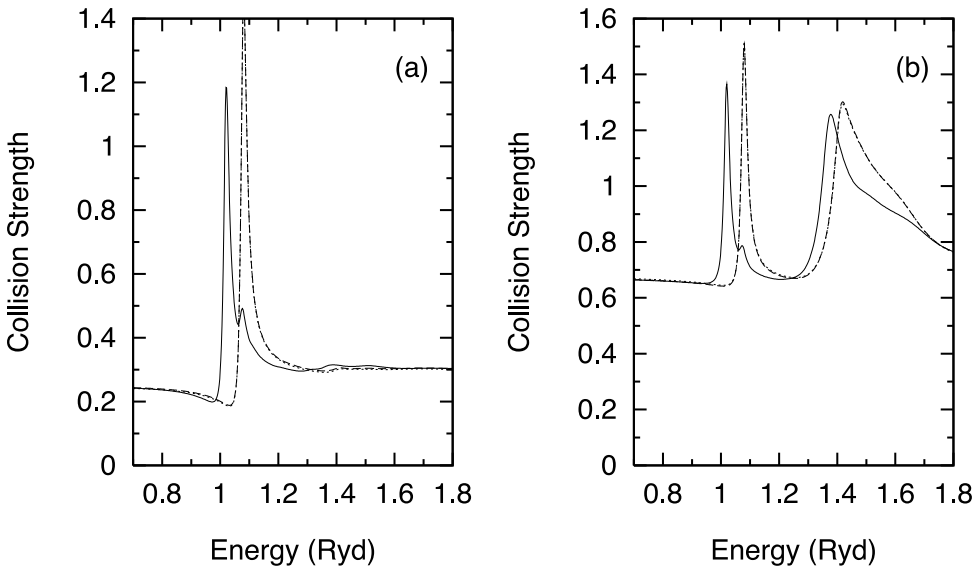

Figure 3. R-matrix electron-impact excitation collision strengths for the transitions (*a*) $^5D_4-^3P_2$ and (*b*) $^5D_4-^3H_6$ in Ni^{4+}. Full curve, Breit–Pauli; dashed curve, ICFT; dotted curve, jK-coupling.

that are not modelled by the ICFT method—recall, no frame transformation is applied to the correlation resonances. (The 3p spin–orbit parameter is a factor 14 larger than the 3d.) The splitting is more evident in the results for the $^5D_2-^3P_2$ and $^5D_2-^3H_6$ transitions, which we compare in figure 4. The difference between our jK-coupling and ICFT results is a little greater than for transitions from the $^5D_4$ ground level but the Breit–Pauli results exhibit a much stronger redistribution of the resonance strength.

Next, in figure 5, we compare our results from the three methods for the $^5D_4-^3H_4$ and $^5D_4-^3F_4$ transitions. Here we see that the jK-coupling results fail completely, both for the background and the resonance strength. We recall from section 3 that the $^3H_4$ and $^3F_4$ levels are strongly (spin–orbit) mixed. This effect is well represented by the ICFT method, as a

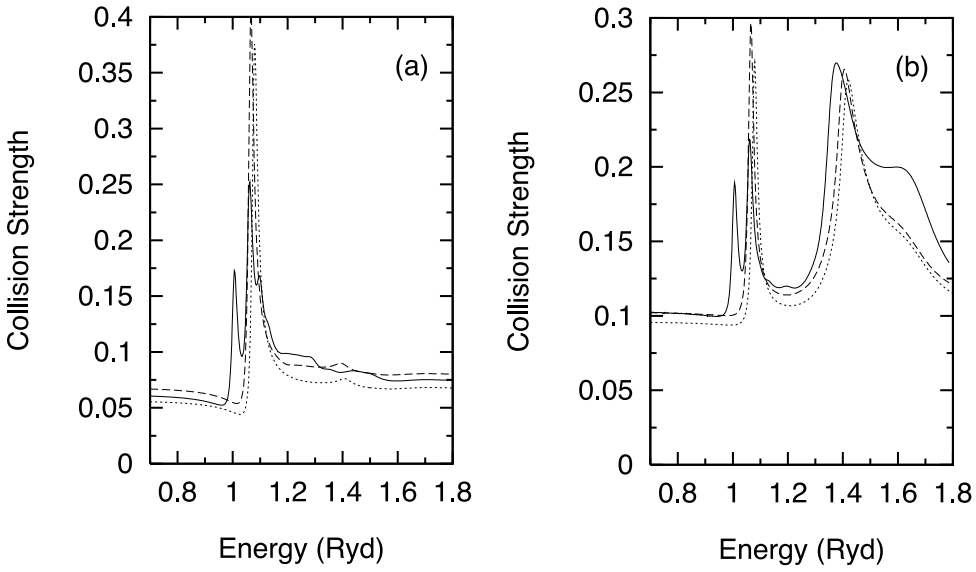

Figure 4. *R*-matrix electron-impact excitation collision strengths for the transitions (*a*) $^5D_2-^3P_2$ and (*b*) $^5D_2-^3H_6$ in Ni^{4+}. Full curve, Breit–Pauli; dashed curve, ICFT; dotted curve, *jK*-coupling.

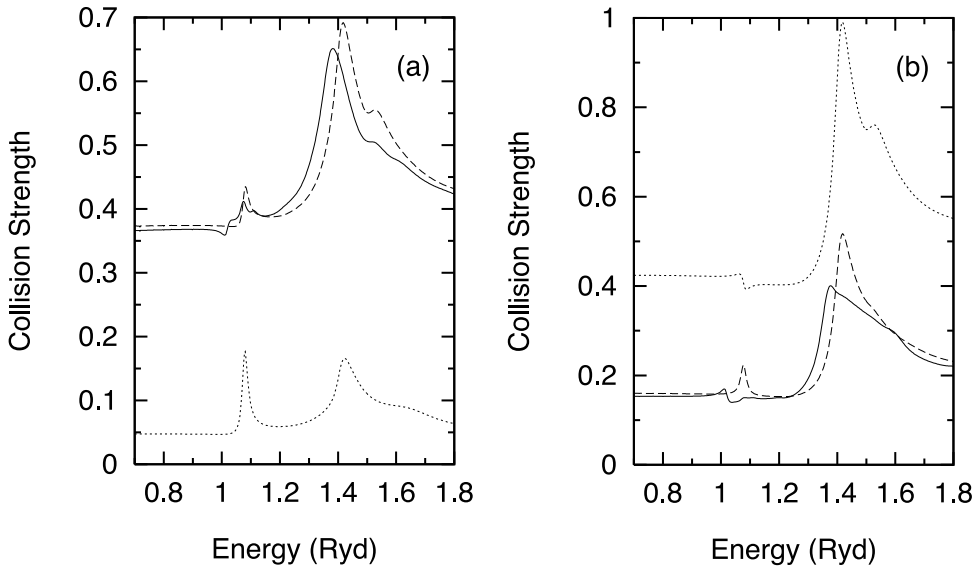

Figure 5. *R*-matrix electron-impact excitation collision strengths for the transitions (*a*) $^5D_4-^3H_4$ and (*b*) $^5D_4-^3F_4$ in Ni^{4+}. Full curve, Breit–Pauli; dashed curve, ICFT; dotted curve, *jK*-coupling.

comparison of the background with the Breit–Pauli result shows, but it is not modelled by the *jK*-coupling method (of course). The ICFT and Breit–Pauli resonance strength is again redistributed a little.

So far, the differences between the results of the ICFT and Breit–Pauli methods are mainly redistributive, and would therefore have a small effect on the total rate coefficients. We now give an example where this may not be the case. In figure 6, we compare our results for

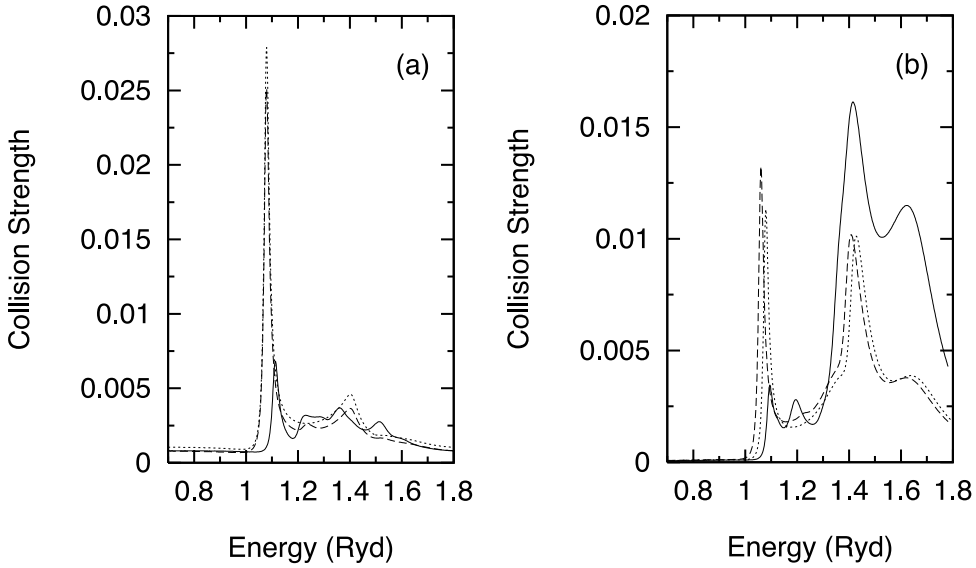

Figure 6. *R*-matrix electron-impact excitation collision strengths for the transitions (*a*) $^5D_4-{}^3P_0$ and (*b*) $^5D_0-{}^3H_6$ in Ni^{4+}. Full curve, Breit–Pauli; dashed curve, ICFT; dotted curve, *jK*-coupling.

the $^5D_4$–$^3P_0$ and $^5D_0$–$^3H_6$ transitions. These are extremely weak transitions ($\Delta J = 4$ and 6, respectively) both for the non-resonant background and resonance contributions. We see that the Breit–Pauli resonance strength is a factor of $\sim$2 smaller (larger) for the first (second) transition. However, one would not normally base a diagnostic on such weak transitions.

5. Conclusions

The results that we have presented here are illustrative of those that we have observed in Ni^{4+}. But, we have tended to focus on the worst cases. For example, for transitions between fine-structure levels of a given term, we observed very small differences between the ICFT and Breit–Pauli results and so we did not present them here. Except for a few extremely weak transitions, the correlation resonances can be expected to contribute at most 10% to the rate coefficients between levels, based on the *LS*-coupling results of Teng *et al* (1998). Even for systems where the correlation resonances may make a somewhat larger contribution to the rate coefficient, the redistributive nature of the Breit–Pauli results compared with the ICFT means that the ICFT method should be more than accurate enough for plasma diagnostics. Only for comparison with precise measurements or for a detailed analysis of autoionizing resonances is a full Breit–Pauli treatment necessary, and then only in energy regions where such correlation resonances are present.

Acknowledgment

In this work, DCG was supported by a US DoE grant (DE-FG02-96-ER54367) with Rollins College.

References

Aymar M, Greene C H and Luc-Koenig E 1996 *Rev. Mod. Phys.* **68** 1015–123
Badnell N R 1986 *J. Phys. B: At. Mol. Phys.* **19** 3827–35
Badnell N R, Gorczyca T W and Price A D 1998 *J. Phys. B: At. Mol. Opt. Phys.* **31** L239–48
Bartschat K, Hudson E T, Scott M P, Burke P G and Burke V M 1996 *J. Phys. B: At. Mol. Opt. Phys.* **29** 115–23
Berrington K A, Burke P G, Butler K, Seaton M J, Storey P J, Taylor K T and Yu Yan 1987 *J. Phys. B: At. Mol. Phys.* **20** 6379–97
Berrington K A, Eissner W B and Norrington P H 1995 *Comput. Phys. Commun.* **92** 290–420
Bray I and Stelbovics A T 1992 *Phys. Rev.* A **46** 6995–7011
Burke P G, Burke V M and Dunseath K M 1994 *J. Phys. B: At. Mol. Opt. Phys.* **27** 5341–73
Burke P G and Robb W D 1975 *Adv. At. Mol. Phys.* **11** 143–214
Eissner W, Jones M and Nussbaumer H 1974 *Comput. Phys. Commun.* **8** 270–306
Gorczyca T W, Felfli Z, Zhou H-L and Manson S T 1998 *Phys. Rev.* A **58** 3661–72
Gorczyca T W, Robicheaux F, Pindzola M S and Badnell N R 1996 *Phys. Rev.* A **54** 2107–15
Greene C H and Kim L 1988 *Phys. Rev.* A **38** 5953–6
Griffin D C, Badnell N R and Pindzola M S 1998 *J. Phys. B: At. Mol. Opt. Phys.* **31** 3713–27
Griffin D C, Badnell N R, Pindzola M S and Shaw J A 1999 *J. Phys. B: At. Mol. Opt. Phys.* **32** at press
Jones M 1975 *Phil. Trans. R. Soc.* A **277** 587–622
Kelly R L 1987 *J. Phys. Chem. Ref. Data* **16** suppl. 1
Lecomte J-M, Telmini M, Aymar M and Luc-Koenig E 1994 *J. Phys. B: At. Mol. Opt. Phys.* **27** 667–97
Seaton M J 1983 *Rep. Prog. Phys.* **46** 167–257
——1985 *J. Phys. B: At. Mol. Phys.* **18** 2111–31
Teng H, Watts M S, Burke V M and Burke P G 1998 *J. Phys. B: At. Mol. Opt. Phys.* **31** 1355–66